Research Paper

Performance and Characterizations of [EMIM][Tf$_2$N] and Silica Direct Blending in Mixed Matrix Membrane for CO$_2$/CH$_4$ Separation

Siti Nur Alwani Shafie [1], Muhammad Amirul Mukmin Marzuki [1], Nik Abdul Hadi Md Nordin [1,*], Muhammad Roil Bilad [1], Norazlianie Sazali [2], Noor Maizura Ismail [3], Ahmad Fauzi Ismail [4]

[1] Department of Chemical Engineering, Universiti Teknologi PETRONAS (UTP), 32610 Seri Iskandar, Perak Darul Ridzuan, Malaysia
[2] Faculty of Mechanical Engineering, Universiti Malaysia Pahang (UMP), 26600 Pekan, Pahang Darul Makmur, Malaysia
[3] Faculty of Engineering, Universiti Malaysia Sabah, Jalan UMS, 88400 Kota Kinabalu, Sabah, Malaysia
[4] Advanced Membrane Technology Research Centre (AMTEC), Universiti Teknologi Malaysia, 81310 Skudai, Johor Darul Takzim, Malaysia

Article info

Keywords

Highlights

- No agglomeration effect with the incorporation of IL
- Presence of low loading of IL has increase the CO$_2$ permeability and CO$_2$/CH$_4$ selectivity compared to that of pure PC
- IL act as the bridging agent and improves PC and silica interaction

Graphical abstract

Abstract

Ionic liquids (ILs) have been studied for CO$_2$ capture owing to the excellent properties of having high CO$_2$ affinity and negligible vapor pressure. The incorporation of IL in polycarbonate (PC) based Mixed Matrix Membrane (MMM) is becoming one of the promising approaches for developing membrane for CO$_2$/CH$_4$ separation. Silica nanoparticle has also been proven to improve performance of MMM for CO$_2$/CH$_4$ separation. Thus, this study investigates the effect of direct blending of IL (1-ethyl-3-methylimidazolium bis(trifluoromethylsulfonyl)imide, [EMIM][Tf$_2$N]) and silica into the MMM on its properties and CO$_2$/CH$_4$ separation performances. The immobilization of silica particles and [EMIM][Tf$_2$N] was confirmed from the FTIR peaks data. The IL in the MMM significantly increases the MMM rigidity as ascribed by its enhanced glass transition temperature. The IL in the MMM improves the interaction by acting as a bridging agent between silica particles and PC. The MMM with 1 wt% of fillers and IL shows the highest performance by enhancing CO$_2$ permeability by 13 folds and selectivity by 35% compared to that of pure PC membrane. The results suggest that low loading of silica/IL in MMM is noteworthy to be explored and further studies at high loading are warranted.
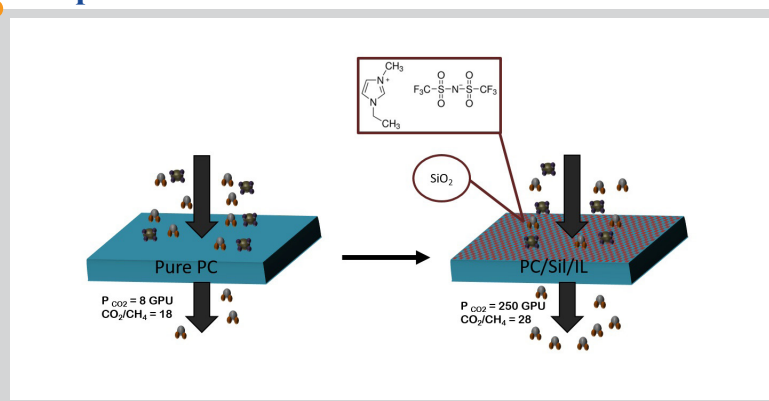
1. Introduction

Ionic liquid (IL) has been receiving attention as the new material for handling carbon dioxide (CO$_2$) separation due to the unique properties of being non-volatile, inflammable and highly selective towards CO$_2$ [1-3]. Studies have shown that imidazolium based IL has high CO$_2$ solubility [4,5]. Cedena et al. [6] reported that CO$_2$ is very soluble in imidazolium anion especially bis(trifluoromethylsulfonyl)-imide, tetrafluoroborate and hexafluorophosphate. The CO$_2$ solubility is affected by two factors; the presence of hydrogen molecule on the C$_2$ and the dominant factor which is the presence of fluoroalkyl groups that has strong affinity to CO$_2$. The [Tf$_2$N] anion have two flouroalkyl groups, thus when presents, leading to ILs with high CO$_2$ solubility.

The ILs superior attributes of high CO$_2$ solubility attract their utilization

for CO_2 separation, such as supported ionic liquid membrane (SILM) [7-11] and polymer-ionic liquid membrane [12]. Chen et al. [13] studied the separation performance of CO_2/H_2 and CO_2/CH_4 using polyvinylidene difluoride IL blend membrane. Both permeability and selectivity increased at higher IL content. The CO_2 permeability increment is prominent owing to the increase in both CO_2 diffusivity and solubility attributed by IL. Increasing IL loading enhances the fractional free volumes (FFV), leading to higher gas diffusivity and permeability.

Incorporation of IL in MMM has been recently investigated [14-16]. Hudiono et al. [14] reported that MMM/ILs has higher permeabilities of CO_2, CH_4 and N_2 by 63%, 40% and 48%, respectively compared to the neat polymerizable room-temperature ionic liquids (poly(RTIL)) membrane. The selectivity of both CO_2/CH_4 and CO_2/N_2 also increase by 11% indicating the great potential of IL blend membranes in CO_2 separation. Furthermore, 1-ethyl-3-methylimidazolium bis(trifluoromethylsulfonyl)imide ([EMIM][Tf$_2$N]) has shown incredible result in CO_2 solubility as high as 60 mol% [17], showing its potential to be used in membrane for CO_2 separation. Hence, direct blending of ILs in MMM has been proven as an effective way to enhance gas separation performance.

It should be noted that the previous work on MMM-IL focuses on utilizing porous filler that highlighted improvement on the molecular sieving effect with IL presence [14,15], whereas there is still limited study on utilizing non-porous filler. The objective of this work is to investigate the effect of three components blending between ionic liquid, polymer and inorganic filler on the properties of the MMM-IL membrane and the CO_2/CH_4 separation performance. The novel aspect of this work is on the incorporation of [EMIM][Tf$_2$N] in PC/Silica MMM in which the [Tf$_2$N] anion in the IL is expected to increase the CO_2 affinity.

2. Experimental

2.1. Materials

CALIBRE™ polycarbonate (PC) was purchased from LG-Dow Ltd, dicholoromethane (DCM), tetraethylorthosilicate (TEOS), hydrochloric acid (HCl, 37%) and ethanol (EtOH)(99.5% purity) were purchased from Merck. The IL of [EMIM][TF$_2$N] was procured from Sigma-Aldrich. All chemicals were used without further purification.

2.2. Silica particles synthesis

Silica particles were synthesized using the standard sol-gel process for non-porous silica [18]. TEOS (30 mL) was hydrolyzed in the presence of EtOH (31 ml) for 5 minutes under reflux at 60 °C. A mixture of 31 ml of distilled water and 0.1 ml of HCl was gradually added and further stirred for 90 minutes. The reaction mixture was then cooled to room temperature before dried in an oven at 60 °C overnight. The silica particles were then washed with distilled water followed by 200 ml of EtOH before filtered and later dried in a vacuum oven at 105 °C overnight.

2.3. Fabrication of mixed matrix membrane

All MMMs were prepared using the same process based on the composition tabulated in Table 1. Silica particles and IL is kept equal, adapted from work by Li et al. [15]. For the dope solutions preparation, 5 g of PC pellets was added into a schott bottle followed by 20 g of DCM. A fixed amount (Table 1) of silica particles and [EMIM][TF$_2$N] IL was added into the membrane solution. After mixing overnight, the mixture was sonicated for few hours to remove trapped air bubbles and to minimize the particle agglomeration. The mixture was poured on dry flat glass surface and manually casted with thickness of approximately 100 µm. The membrane sheet was let dry for 24 h enclosed environment to ensure complete solvent evaporation.

2.4. Characterizations

Fourier Transform Infrared Spectrometer (FTIR) analysis was done to determine the functional group changes of silica powder after blending with [EMIM][TF$_2$N]. The analysis was done using Perkin-Elmer Spectrum 1 Fourier transform Infrared spectrometer and the spectra were analyzed by the Spectra One Software. The powder sample and KBr were grounded before mixing. The mixture powder was then added into a die-set to form a pellet before placed in the sample holder. The spectrum was studied by co-addition of 20 scans in the range of 400-4000cm^{-1}. Within this range, the organic component converted the radiation into vibration.

The morphology of fabricated membranes was analyzed using field emission scanning electron microscopy (FESEM). The membranes were fractured in liquid nitrogen and mounted on carbon-taped holder before coated in gold/platinum. All membranes were analyzed at magnification range of 2k to 3k using 15kV accelerating voltage.

Thermal gravimetric analyzer (TGA, Perkin Elmer) was carried out to anayze the thermal stability, material composition and purity and the amount of residual solvent in the MMMs after drying. For this analysis, the MMMs were heated at temperature range of 25- 800 ºC at 10 ºC /min heating rate under nitrogen condition.

Differential scanning calorimetry (DSC) was used to analyze the effect silica/IL blending into the MMMs from the glass transition temperature (T$_g$) data. Firstly, small cuts and cleaned MMMs were placed on the DSC pans. The samples were heated from 30 ºC to 800 ºC at a rate of 10 ºC /min in N$_2$ condition. After reaching 250 ºC, the samples were naturally cooled to remove the thermal history. Under the same procedure, the second scan was conducted again. To get the T$_g$ value of the MMMs, the second scan values were referred.

2.5. Gas permeation test

The gas permeation was conducted using pure CO_2 and CH_4 gas under feed pressure range of 4-10 bar at room temperature (25 ºC). CH_4 was tested first to avoid membrane plasticization by CO_2 and the flowrate of gas permeated was measured using bubble flow meter. The permeance, P/l (unit GPU), is then calculated using the following equation:

$$\frac{P}{l} = \frac{Q_{STP}}{A.\Delta P} \tag{1}$$

where Q_{STP} is the permeate flow rate at standard temperature and pressure. A is the effective surface area of the membrane film, ΔP is the pressure gradient across the membrane. The unit of gas permeance is expressed in GPU (Eq. 2).

$$GPU = 1 \times 10^{-6} \frac{cm^3 (STP)}{sec.cm^2.cmHg} \tag{2}$$

The gas pair selectivity of a membrane was evaluated by permeability ratio of the more permeable gas over the less permeable gas (CO_2/CH_4). The separation factor was defined as in Eq. 3.

$$\alpha_{CO_2/CH_4} = \frac{(P/l)_{CO_2}}{(P/l)_{CH_4}} \tag{3}$$

3. Results and discussions

3.1. Sample characterization

The FTIR spectra for all prepared samples are presented in Figure 1. Intense wavelength range 1100-1200 cm^{-1} reflected the Si-O-Si asymmetric stretching [19]. These observations confirm that silica was successfully synthesized. Upon incorporating the synthesized silica and the IL into the PC matrix, peaks at 900 cm^{-1} represents imidazolium ring and at 1300 cm^{-1} represents S=O bond from the anion of [EMIM][TF$_2$N]. This indicates that the [EMIM][Tf$_2$N] was successfully immobilised within the PC matrix. Increasing the Sil-IL loading does not affect the peak intensity likely due to relatively small step-increased of Sil-IL loading.

Table 1
List of samples and the amount of silica nanoparticles and ionic liquid.

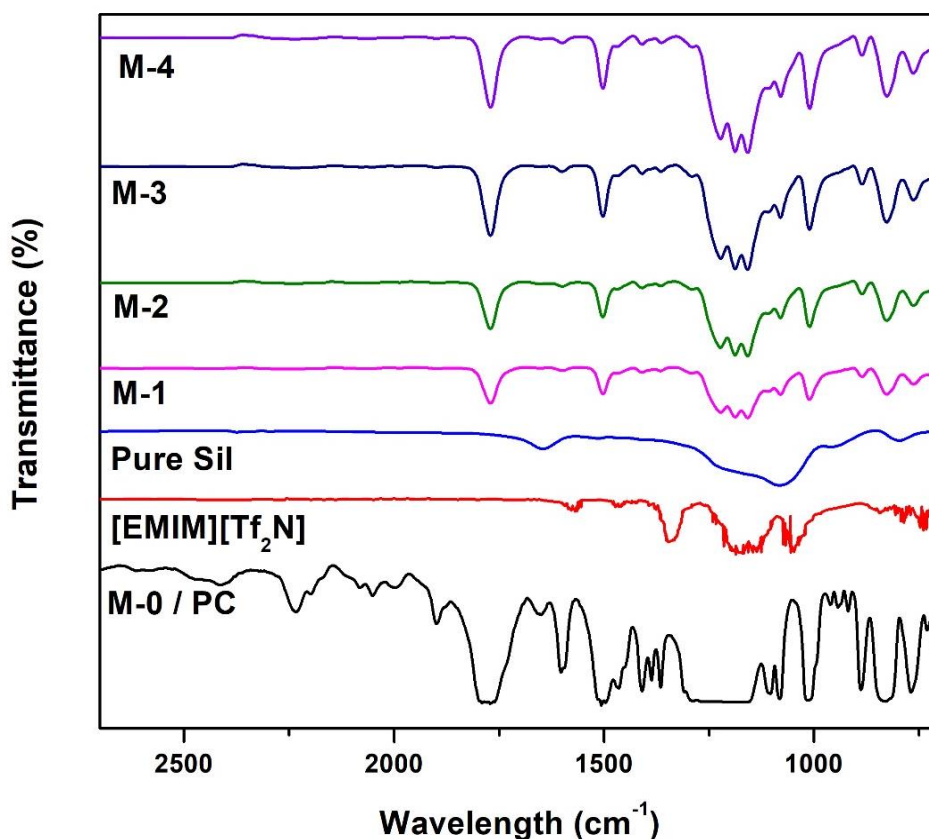| Sample	DCM (wt%)	PC (wt%)	Silica particles (wt% based on the weight of polymer)	[EMIM][TF$_2$N] (wt% based on the weight of polymer)
M-0	80	20	-	-
M-1	80	20	1	1
M-2	80	20	2	2
M-3	80	20	3	3
M-4	80	20	4	4

Fig. 1. FTIR spectra for pure PC, [EMIM][TF$_2$N] adapted from [20], pure Sil (silica particle) fillers and the fabricated MMMs.

The cross-sectional morphologies of the developed MMMs were shown in Figure 2. The M-0 poses dense morphology, which is expected from slow solvent evaporation during membrane preparation. In contrast to the M-0, the incorporation of silica has induced some morphological changes (Figure 2b-e) on the rest on the MMM samples. Some non-selective voids present as silica particles disrupt the polycarbonate chain. Additionally, no agglomeration of the silica particles can be observed likely because of low amount of Silica loadings.

The presence of the incorporated IL/silica into the PC matrix are identified from the SEM-EDX (Figure 3) and summarized in Table 2. The EDX analysis was conducted to identify the distribution of Silica particles and [EMIM][Tf$_2$N]. The C element (%) represents the polymer phase, Si element (%) represents silica particles, and F element (%) represents the IL [EMIM][Tf$_2$N]. It should be noted that the mapping was done specifically on the silica particle, hence the Si (%) atomic element is significantly higher that its loading. Small amount of F element presents for all MMM/ILs indicating the present of IL.

Table 3 shows the T$_g$ of all developed MMMs. Interestingly, upon incorporation of IL, significant increase in the T$_g$ was observed. The increased in T$_g$ value indicates that the MMMs become more rigid [21,22]. The increased in T$_g$ upon incorporating IL suggests that IL acts as bridging agent between PC and silica, indicating a strong interaction thus increases the rigidity of the polymer matrix. Therefore, the rigidification of the polymer is mainly due to the addition of IL. However, further increases the Silica-IL loading at 4wt% resulting slight decrease in membrane's T$_g$, likely due to the IL-induced plasticization. Similar observation also observed by Zheng *et al.* [23] where low IL loading promotes chain stiffening in polymer matrices due to good polymer-IL interaction, whereas, high IL loading would promotes IL-induces plasticization.

3.2. Gas separation performance

The permeation results of all MMMs using pure CO$_2$ and pure CH$_4$ as the feed are presented in Figure 4. The CO$_2$ permeance and CO$_2$/CH$_4$ selectivity of M-0 are 8.3 GPU and 18.1, respectively, which fall within earlier reported values [24]. The M-1 shows an increment of 7 folds of CO$_2$ permeance (256.6 GPU) compared to M-0. Although the increase in T$_g$ (Table 3) would

typically indicate the decrease in CO$_2$ permeance due to rigidification of polymer, gas permeation shows an increase in CO$_2$ permeance. The increase in CO$_2$ permeance can be attributed to higher CO$_2$ solubility due to the presence of IL. Furthermore, the localization of IL in the polymer matrix creates FFV that promotes CO$_2$ permeation.

Table 2
EDX atomic analysis of cross-section morphology for the polymer/silica/IL blend.

Sample	Element (atomic %)		
	C	F	Si
M-1	93.08	0.90	6.02
M-2	97.54	0.30	2.15
M-3	87.10	0.04	12.87
M-4	92.39	0.57	7.05

Table 3
Glass transition temperature (T$_g$) of all developed membranes.

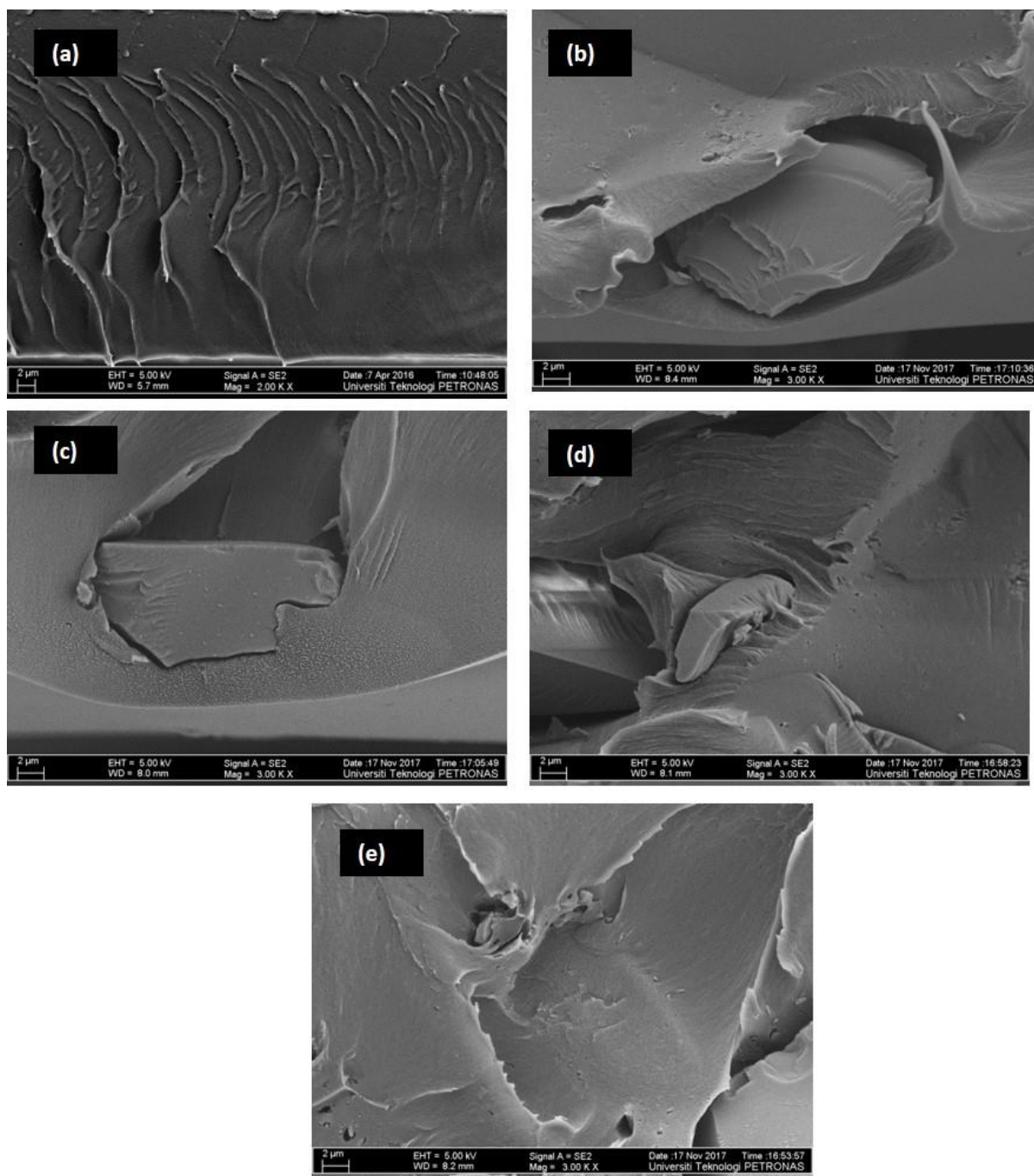| Membranes	T$_g$ (ºC)
M-0	144.4
M-1	146.8
M-2	146.5
M-3	147.5
M-4	146.3

Fig. 2. FESEM images of a) M-0, b) M-1, c) M-2, d) M-3, e) M-4.

Interestingly, for MMMs with additions of 2-4 wt% of Silica/IL (M-2, M-3 and M-4), their permeances are lower than M-1, albeit higher than M-0. The decrease in CO_2 permeance can be attributed to the dominant IL's role as the bridging agent (Table 3) which further rigidifying the PC polymer. The CO_2/CH_4 selectivity of the developed MMMs follows similar trend of the CO_2 permeance. Although, the role of IL as the bridging agent is attributed to dictate the CO_2 permeance, it is difficult to draw the same conclusion for CO_2/CH_4 selectivity. As the loading increase, the presence of IL should increase the CO_2/CH_4 selectivity. However, Figure 4 shows a steep decrease of the CO_2/CH_4 selectivity. Such trend can be explained by the dominant role of silica which creates non-selective voids that facilitate increasing permeance of both gases thus reducing the selectivity.

Figure 5 shows the effect of pressure on the gas separation performances. All membrane samples were tested at different pressure ranging 4 -10 bar. For M-0, CO_2 permeance (Figure 5a) shows decreasing trend with increasing pressure, obeying the dual-mode sorption model. As pressure increases, the

FFV become saturated, reducing the pathway for gas permeation thus the decreasing permeance. However, for M-1 and M-2, the CO_2 permeance increases from 4-8 bar pressure before dropping when approaching 10 bar. Meanwhile, for M-3 and M-4, the CO_2 permeance increases at higher pressures. The trend indicates that all MMM/ILs has reached the plasticization point where the membrane swells upon the sorption of CO_2 as the pressure increase.

Figure 5b shows the effect of pressure on CO_2/CH_4 selectivity. M-0 shows slight decrease in the selectivity, while M-1 shows prominent decrease as the pressure increase due to drop in CO_2 permeance at higher pressure (Figure 5a). Similar to M-1, M-2 also shows decrement in CO_2/CH_4 selectivity as the pressure increases. M-3 and M-4 show decreasing CO_2/CH_4 selectivity as well although capping at much lower value than that of M-0 and M-1. The decrease in selectivity is precedent due to the increase in gas permeability. As the pressure increase, the polymer swells upon the sorption of CO_2 which diminished the gas selectivity.
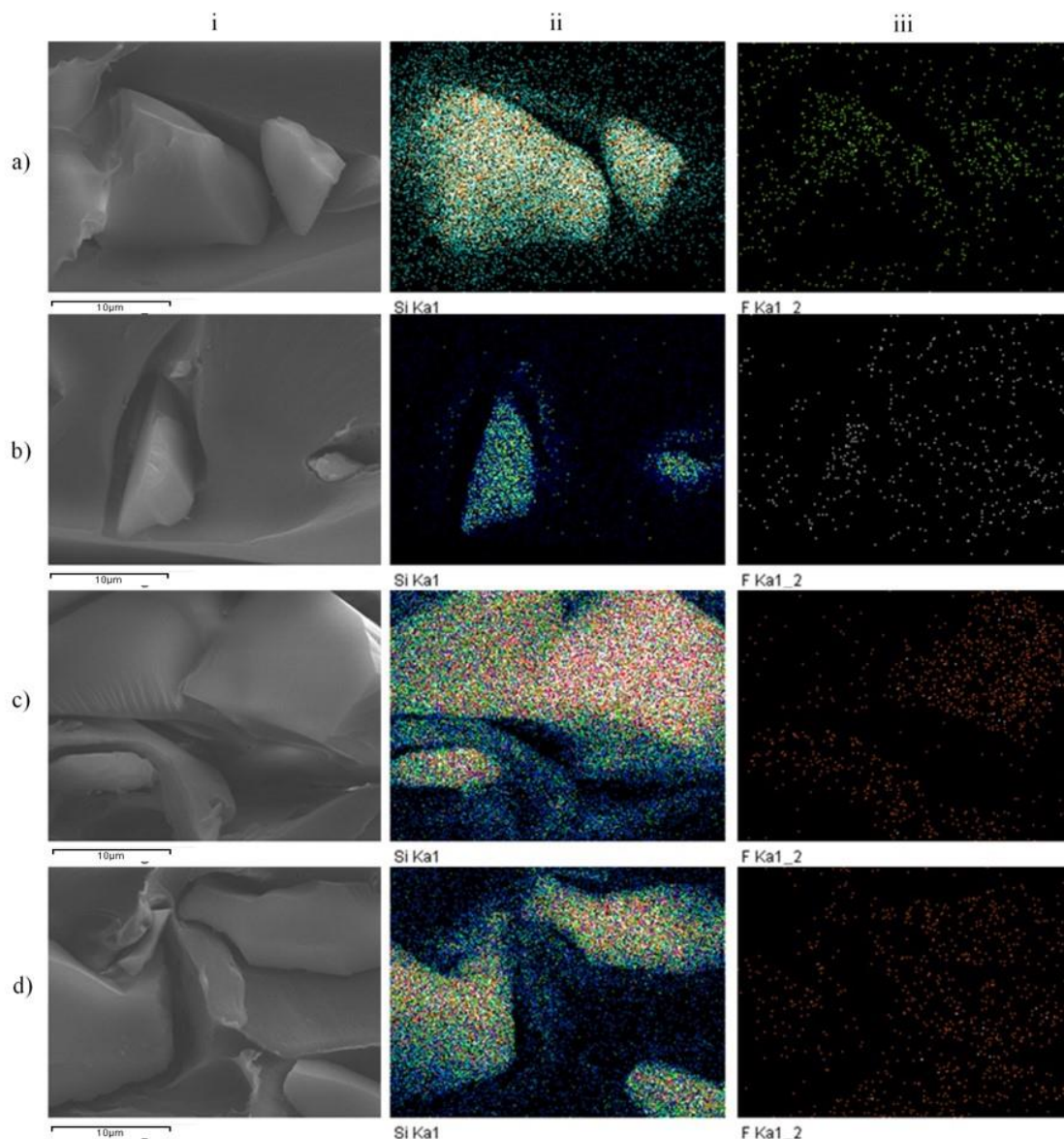
Fig. 3. EDX analysis of cross-section morphology for a) M-1, b) M-2, c) M-3, and d) M-4, with i) SEM images, ii) Si atomic element, and iii) F atomic element.

4. Conclusions

The effects of silica fillers and IL blending on PC membrane were investigated. Polycarbonate incorporated with different loadings of silica/IL [EMIM][Tf$_2$N] were successfully fabricated as indicated by the presence of silica and IL associated FTIR peaks and EDX atomic analysis. The incorporation of silica and [EMIM][TF$_2$N] IL promote formation of voids, without obvious formation of agglomerates. The presence of IL MMM increases the T$_g$, and PC rigidity due to its Silica to PC bridging effect. From the permeation test, IL-incorporated membranes (M-1, M-2, M-3 and M-4) show higher CO$_2$ permeance at low pressure compared to the pure PC membrane (M-0) thanks to the role of [EMIM][Tf$_2$N] IL in enhancing CO$_2$ affinity. However, with increasing pressure, the CO$_2$ increase while the selectivity falls below of that of M-0. This indicates that the developed MMMs have pose low plasticization pressure. It is also noted that, among all developed MMM/ILs, M-1 shows the promising performance with CO$_2$ permeance of 256.6 GPU with CO$_2$/CH$_4$ selectivity of 28 at 4 bar. Although the incorporation of [EMIM][Tf$_2$N] has shown improvement in gas separation performance, further study on the plasticization effect should be considered in the future The separation behavior of the MMMs based on the effect of one of filler (silica filler or IL) while keeping constant the loading of the other should be studied to further understand the effect of fillers on MMM gas separation performance.
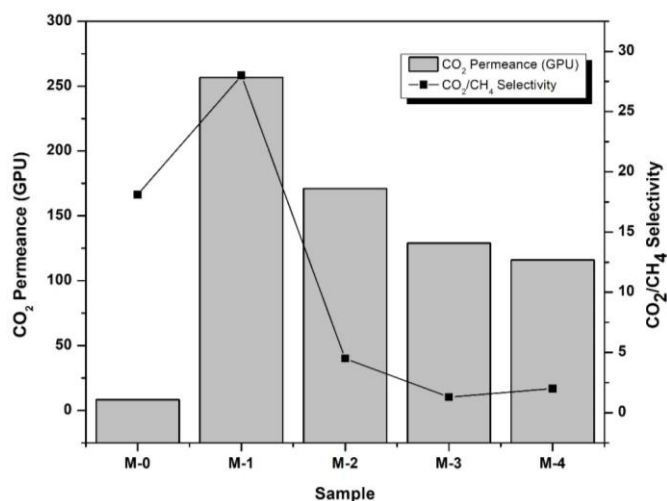

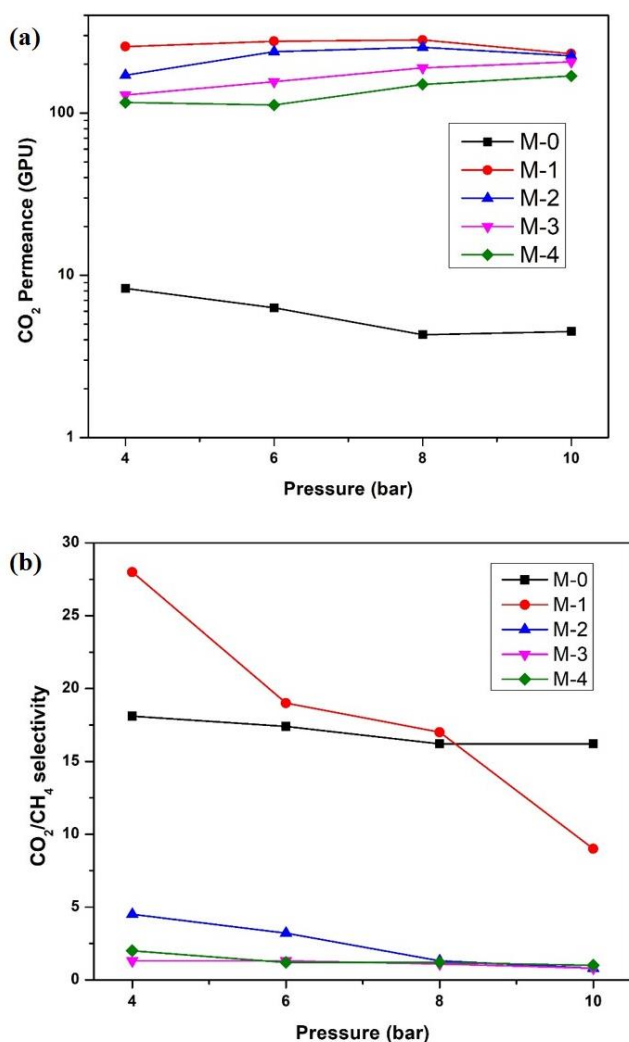**Fig. 4.** Gas permeation performance of prepared membranes at feed pressure of 4 bar.

Fig. 5. Effect of feed pressure on (a) CO_2 permeance (b) CO_2/CH_4 selectivity data for all membranes.

Acknowledgement

References

[1] E.D. Bates, R.D. Mayton, I. Ntai, J.H. Davis, CO_2 capture by a task-specific ionic liquid, J. Am. Chem. Soc., 124 (2002) 926-927, doi: 10.1021/ja017593d.

[2] B. Gurkan B.F. Goodrich, E.M. Mindrup, L.E. Ficke, M. Massel, S. Seo, T.P. Senftle, H. Wu, M.F. Glaser, J.K. Shah, E.J. Maginn, Molecular design of high capacity, low viscosity, chemically tunable ionic liquids for CO_2 capture, J. Phys. Chem. Lett., 1 (2010) 3494-3499,doi: 10.1021/jz101533k.

[3] J. Huang, T. Rüther, Why are ionic liquids attractive for CO_2 absorption? An overview, Aust. J. Chem., 62 (2009) 298-308, doi: https://doi.org/10.1071/CH08559.

[4] J.L. Anthony, E.J. Maginn, J.F. Brennecke, Solution thermodynamics of imidazolium-based ionic liquids and water, J. Phys. Chem. B, 105 (2001) 10942-10949, doi: 10.1021/jp0112368.

[5] L.A. Blanchard, Z. Gu, J.F. Brennecke, High-pressure phase behavior of ionic liquid/CO_2 systems, J. Phys. Chem. B, 105 (2001) 2437-2444, doi: 10.1021/jp003309d.

[6] C. Cadena, J.L. Anthony, J.K. Shah, , T.I. Morrow, J.F. Brennecke, E.J. Maginn, Why is CO_2 so soluble in imidazolium-based ionic liquids?, J. Am. Chem. Soc., 126 (2004) 5300-5308, doi: 10.1021/ja039615x.

[7] M.Y.M. Abdelrahim, C.F. Martins, L.A. Neves, C. Capasso, C.T. Supuran, I.M. Coelhoso, J.G. Crespo, M. Barboiu,, Supported ionic liquid membranes immobilized with carbonic anhydrases for CO_2 transport at high temperatures, J. Membr. Sci., 528 (2017) 225-230, doi: https://doi.org/10.1016/j.memsci.2017.01.033.

[8] J.J. Close, K. Farmer, S.S. Moganty, R.E. Baltus, CO_2/N_2 separations using nanoporous alumina-supported ionic liquid membranes: Effect of the support on separation performance, J. Membr. Sci., 390-391 (2012) 201-210, doi: https://doi.org/10.1016/j.memsci.2011.11.037.

[9] E. Santos, J. Albo, A. Irabien, Acetate based supported ionic liquid membranes (SILMs) for CO_2 separation: Influence of the temperature, J. Membr. Sci., 452 (2014) 277-283, doi: https://doi.org/10.1016/j.memsci.2013.10.024.

[10] D.S. Karousos, A.I. Labropoulos, A. Sapalidis, N.K. Kanellopoulos, B. Iliev, T.J. Schubert, G.E. Romanos, Nanoporous ceramic supported ionic liquid membranes for CO_2 and SO_2 removal from flue gas, Chem. Eng. J., 313 (2017) 777-790, doi: https://doi.org/10.1016/j.cej.2016.11.005.

[11] X. Zhang Z. Tu, H. Li, K. Huang, X. Hu, Y. Wu, D.R. MacFarlane, Selective separation of H_2S and CO_2 from CH_4 by supported ionic liquid membranes, J. Membr. Sci., 543 (2017) 282-287, doi: https://doi.org/10.1016/j.memsci.2017.08.033.

[12] J. Yuan, D. Mecerreyes, M. Antonietti, Poly(ionic liquid)s: An update,"Prog. Polym Sci., 38 (2013) 1009-1036, doi: https://doi.org/10.1016/j.progpolymsci.2013.04.002.

[13] H.Z. Chen, P. Li, T.S. Chung, PVDF/ionic liquid polymer blends with superior separation performance for removing CO_2 from hydrogen and flue gas, Int. J. Hydrogen Energ., 37 (2012) 11796-11804, doi: https://doi.org/10.1016/j.ijhydene.2012.05.111.

[14] Y.C. Hudiono, T.K. Carlisle, J.E. Bara, Y. Zhang, D.L. Gin, R.D. Noble, A three-component mixed-matrix membrane with enhanced CO_2 separation properties based on zeolites and ionic liquid materials, J. Membr. Sci., 350 (2010) 117-123, doi: https://doi.org/10.1016/j.memsci.2009.12.018.

[15] H. Li, L. Tuo, K. Yang, H.K. Jeong, Y. Dai, G. He, W. Zhao, Simultaneous enhancement of mechanical properties and CO_2 selectivity of ZIF-8 mixed matrix membranes: Interfacial toughening effect of ionic liquid, J. Membr. Sci., 511 (2016) 130-142, doi: https://doi.org/10.1016/j.memsci.2016.03.050.

[16] S.N.A. Shafie, W.. Liew, N.A.H. Md Nordin, M.R. Bilad, N. Sazali, Z.A. Putra, M.D.H. Wirzal, CO_2-Philic [EMIM][Tf_2N] Modified silica in mixed matrix membrane for high performance CO_2/CH_4 separation, Adv. Polym. Technol., 2019 (2019) 2924961, doi: 10.1155/2019/2924961.

[17] A.M. Schilderman, S. Raeissi, C.J. Peters, Solubility of carbon dioxide in the ionic liquid 1-ethyl-3-methylimidazolium bis(trifluoromethylsulfonyl)imide, Fluid Phase Equilibr., 260 (2007) 19-22, doi: https://doi.org/10.1016/j.fluid.2007.06.003.

[18] A.M. Buckley, M. Greenblatt, The sol-gel preparation of silica gels, J. Chem. Educ., 71 (1994) 599, doi: 10.1021/ed071p599.

[19] M.E. Mahmoud, Surface loaded 1-methyl-3-ethylimidazolium bis(trifluoromethylsulfonyl)imide [EMIM+$Tf_2N^−$] hydrophobic ionic liquid on nano-silica sorbents for removal of lead from water samples, Desalination, 266 (2011) 119-127, doi: https://doi.org/10.1016/j.desal.2010.08.011.

[20] R.S. Booth, C.J. Annesley, J.W. Young, K.M. Vogelhuber, J.A. Boatz, J.A. Stearns, Identification of multiple conformers of the ionic liquid [EMIM][TF_2N] in the gas phase using IR/UV action spectroscopy, Phys. Chem. Chem. Phys., 18 (2016) 17037–17043, doi: doi:10.1039/c6cp02657e

[21] N.A.H.M. Nordin, A.F. Ismail, A. Mustafa, R.S. Murali, T. Matsuura, The impact of ZIF-8 particle size and heat treatment on CO_2/CH_4 separation using asymmetric mixed matrix membrane, RSC Adv., 4 (2014) 52530-52541, doi: 10.1039/C4RA08460H.

[22] N.A.H. Md Nordin, S.M. Racha, T. Matsuura, N. Misdan, N.A.A. Sani, A.F. Ismail, A. Mustafa, Facile modification of ZIF-8 mixed matrix membrane for CO_2/CH_4 separation: Synthesis and preparation, RSC Adv., 5 (2015) 43110-43120, doi: 10.1039/c5ra02230d.

[23] X. Zheng, Q. Lin, P. Jiang, Y. Li, J. Li, Ionic liquids incorporating polyamide 6: Miscibility and physical properties, Polymers, 10 (2018) 562.

[24] A. Idris, Z. Man, A.S. Maulud, Polycarbonate/silica nanocomposite membranes: Fabrication, characterization, and performance evaluation, J. Appl. Polym. Sci., 134 (2017) 45310, doi: 10.1002/app.45310.